OXFORD

ORIGINAL ARTICLE

Structural Variability Across the Primate Brain: A Cross-Species Comparison

Paula L. Croxson[1], Stephanie J. Forkel[2,3], Leonardo Cerliani[4,5] and Michel Thiebaut de Schotten[4,5]

[1]Friedman Brain Institute, Icahn School of Medicine at Mount Sinai, 1 Gustave L Levy Place, New York, NY 10029, USA, [2]Centre for Neuroimaging Sciences, Department of Neuroimaging, Institute of Psychiatry, Psychology and Neuroscience, King's College London, London, UK, [3]Natbrainlab, Department Forensics and Neurodevelopmental Sciences, Institute of Psychiatry, Psychology and Neuroscience, King's College London, London, UK, [4]Brain Connectivity and Behaviour group, Brain and Spine Institute, Paris, France and [5]Frontlab, Institut du Cerveau et de la Moelle épinière (ICM), UPMC UMRS 1127, Inserm U 1127, CNRS UMR 7225, Paris, France

Address correspondence to Paula L. Croxson, School of Medicine at Mount Sinai, 1 Gustave L Levy Place, New York, NY 10029. Email: paula.croxson@mssm.edu and Michel Thiebaut de Schotten, Institut du cerveau et la moelle épinière. Hôpital de la Salpêtrière—ICM, 47 Bvd de l'Hôpital CS21414, 75646 Paris Cedex 13, France. Email: michel.thiebaut@gmail.com

Abstract

A large amount of variability exists across human brains; revealed initially on a small scale by postmortem studies and, more recently, on a larger scale with the advent of neuroimaging. Here we compared structural variability between human and macaque monkey brains using grey and white matter magnetic resonance imaging measures. The monkey brain was overall structurally as variable as the human brain, but variability had a distinct distribution pattern, with some key areas showing high variability. We also report the first evidence of a relationship between anatomical variability and evolutionary expansion in the primate brain. This suggests a relationship between variability and stability, where areas of low variability may have evolved less recently and have more stability, while areas of high variability may have evolved more recently and be less similar across individuals. We showed specific differences between the species in key areas, including the amount of hemispheric asymmetry in variability, which was left-lateralized in the human brain across several phylogenetically recent regions. This suggests that cerebral variability may be another useful measure for comparison between species and may add another dimension to our understanding of evolutionary mechanisms.

Key words: asymmetry, cross-species comparison, evolution, grey matter, magnetic resonance imaging, variability, white matter

Introduction

Comparative anatomy has revealed that the human brain is greatly enlarged as compared with other primates. This difference in size has been interpreted as an evolutionary expansion (Preuss 2011; Sherwood et al. 2012). However, the critical feature for the evolutionary changes underlying higher cognitive abilities may not be the size of the brain per se, but rather the expansion of some brain regions relative to others (Passingham and Wise 2012; Kaas and Stepniewska 2015). For example, some specific regions of prefrontal cortex and parietal cortex have shown relative expansion or specialization along the evolutionary tree (Semendeferi et al. 2002; Schoenemann et al. 2005; Neubert et al. 2015), combined with a greater degree of lateralization in the human brain (Nathan et al. 1990; Catani et al. 2007, 2010; Thiebaut de Schotten

et al. 2011; Ocklenburg and Gunturkun 2012; Budisavljevic et al. 2015). Despite the importance of individual differences in evolution (Darwin 1859), no studies to date, to our knowledge, have compared inter-individual anatomical variability across species.

Traditionally, comparative anatomy studies have been based on postmortem measures: histological staining, blunt dissections and axonal tracing (Brodmann 1909; Vogt and Vogt 1919; Van Essen et al. 1986; Barbas and Pandya 1987). In recent years, in vivo magnetic resonance imaging (MRI) has become a useful tool not only for the investigation of human brain but also for the direct comparison of human and non-human primate anatomy, both functionally and structurally (Croxson et al. 2005; Vincent et al. 2007; Mars et al. 2011; Mantini et al. 2012; Thiebaut de Schotten et al. 2012). Recent work demonstrates that anatomical inter-individual variability exists within humans with regard to surface anatomy (Whitaker and Selnes 1976; Toga and Thompson 2003; Uylings et al. 2005; Marie et al. 2015), cyto-architectural boundaries (Amunts et al. 1999), connectional anatomy (Catani et al. 2007; Thiebaut de Schotten et al. 2011), and vascular anatomy (van der Zwan et al. 1992). Similar results have been reported for the non-human primate brain (Van Essen and Dierker 2007; Zhang et al. 2013).

Here, we analyzed the amount of structural variability across the human and macaque monkey brain. Our primary hypothesis was that the human brain would be more variable than the macaque monkey brain, particularly in regions that are relatively specialized in humans. Additionally, we hypothesized that a relationship exists between the anatomical variability and the evolutionary expansion in the human brain. These measures were acquired, where possible, with comparable equipment, parameters and resolution between species, in equally sized samples of humans and monkeys, and then analyzed with identical methods.

Materials and Methods

Subjects and MRI Acquisition

Main analysis of T1-weighted images and diffusion-weighted images was obtained from two sets of 10 adult healthy controls (5 males and 5 females per set; age range 26–35 years at the time of data acquisition) from the Human Connectome Project (HCP) (http://www.humanconnectome.org, Q4 Release).

Two additional sets of 16 healthy controls (8 males and 8 females per set; age range 26–35 years at the time of data acquisition) from the HCP (http://www.humanconnectome.org, Q4 Release) were selected to determine the optimal number of participants to build a template.

T1-weighted images and diffusion-weighted images were obtained *in vivo* from 10 healthy rhesus monkeys (*Macaca mulatta*; 6 males and 4 females; age range 3.75–5.82 years at the time of data acquisition; mean 4.5 years). Studies of brain development would place these animals in the category of young adults (Malkova et al. 2006).

HCP Dataset

Data from the HCP dataset were acquired on a Siemens Skyra 3 T scanner at Washington University in St. Louis. The scanner was equipped with a customized body transmitter coil with 56 cm bore size (Van Essen et al. 2013).

T1-Weighted Imaging

An axial three-dimensional (3D) T1-weighted imaging dataset covering the whole head was acquired for each participant (260 slices, voxel resolution = $0.7 \times 0.7 \times 0.7$ mm, TE = 2.14 ms, TR = 2400 ms, flip angle = $8°$).

Diffusion-Weighted Imaging

A total of 111 near-axial slices were acquired with a multiband factor = 3 (Moeller et al. 2010; Ugurbil et al. 2013), isotropic ($1.25 \times 1.25 \times 1.25$ mm) resolution, and coverage of the whole head (TE = 89.5 ms, TR = 5520 ms). At each slice location, 18 images were acquired with no diffusion gradient applied. Additionally, 90 diffusion-weighted images were acquired, in which customized SC72 gradients were uniformly distributed in multiple Q-space shells (Caruyer et al. 2013). The acquisition of the diffusion weighting images was repeated three times with a *b*-value of 1000, 2000, and 3000 s/mm^2. Data were pre-processed using the default HCP pipeline (V.2), which includes correction for susceptibility, motion, and eddy current distortions (Andersson et al. 2012; Sotiropoulos et al. 2013). Pairs of diffusion-weighted volumes were acquired with reversed right-to-left and left-to-right phase-encoding directions. This generates a pair of images where the applied diffusion gradient counterbalances distortions in opposite directions. From these pairs, the susceptibility-induced off-resonance field was estimated using a method similar to that described in Andersson et al. (2003) and corrected on the whole diffusion-weighted dataset using the tool TOPUP as implemented in FSL (Smith et al. 2004). At each slice, diffusion-weighted data were simultaneously registered and corrected for subject motion and geometrical distortion using the tool EDDY as implemented in FSL. Finally, FA maps derived from the volumes with a b-value of 0 and 1000 were computed using DTIFIT (Behrens et al. 2003).

Rhesus Monkey Dataset

Data were collected from the monkeys under anesthesia (protocols described in Mars et al. 2011; Sallet et al. 2011; O'Reilly et al. 2013). Protocols for animal care, MRI, and anesthesia were performed in accordance with the United Kingdom Animals (Scientific Procedures) Act (1986). Anesthesia was induced using ketamine (10 mg/kg intramuscularly; i.m.), xylazine (0.125–0.25 mg/kg i.m.), and midazolam (0.1 mg/kg i.m.) and maintained with isoflurane at a low concentration (0.9–1.7% expired; mean, 1.38%). Anesthesia was supplemented with atropine (0.05 mg/kg, i.m.), meloxicam (0.2 mg/kg, i.v.), ranitidine (0.05 mg/kg, i.v.), and local anesthetic (5% lidocaine/prilocaine cream and 2.5% bupivacaine subcutaneously as necessary). Physiological parameters including capnography, inspired and expired isoflurane concentration, SPO$_2$, core temperature, heart rate, and blood pressure were monitored and kept constant to maintain normal physiological function.

All monkey MRI data were acquired in a 3 T MRI scanner with a full-size horizontal bore and a custom-built 4-channel phased-array coil with a single loop local transmit coil (Windmiller-Kolster Scientific). These data have been used in previous publications (Mars et al. 2011; Sallet et al. 2011; Mars et al. 2013; O'Reilly et al. 2013; Sallet et al. 2013; Neubert et al. 2014; Noonan et al. 2014; Neubert et al. 2015).

T1-Weighted Imaging

T1-weighted images were acquired with a T1-weighted magnetization-prepared rapid-acquisition gradient echo sequence (128 slices, voxel resolution = $0.5 \times 0.5 \times 0.5$ mm, TE = 4.01 ms, TR = 2500 ms). Three images were acquired and subsequently averaged for high signal-to-noise ratio.

Diffusion-Weighted Imaging

Diffusion-weighted images were acquired using echo-planar imaging (56 slices, voxel resolution = 1.0 × 1.0 × 1.0 mm, TE = 102 ms, TR = 8300 ms, acceleration factor = 2). Diffusion weighting was isotropically distributed along 60 directions using a *b*-value of 1000 s/mm^2, with six volumes without diffusion weighting per run. Six averages were acquired per subject; three with left-right phase-encode direction and three with right-left, to facilitate correction for distortions along the phase-encoding direction. As for the human datasets, the susceptibility-induced off-resonance field was estimated (Andersson et al. 2003) and corrected on the whole diffusion-weighted dataset using the tool TOPUP as implemented in FSL followed by registration, motion correction and eddy current correction EDDY (Smith et al. 2004). Finally, FA maps were computed using DTIFIT (Behrens et al. 2003).

Template Reconstruction

In order to quantify the variability, our approach was first to produce an optimal template without spatial priors for each species and modality. We produced these templates using Advanced Normalization Tools (ANTs, http://stnava.github.io/ANTs/) (Avants and Gee 2004; Avants et al. 2010), which build a template iteratively combining affine and diffeomorphic deformations (Avants et al. 2008; Klein et al. 2009). Participants were first aligned together using affine transformation. Then the templates were built from all the subjects iteratively (*n* = 4) using diffeomorphic deformations. Note that to avoid cross modality differences related to the voxel size, T1-weighted images were registered beforehand to FA maps.

Diffeomorphic deformations were performed using the SyN tool in ANTs. The effective resolution of the warp field used was the same as that of the fixed image (1.0 mm^3 in the monkeys and 1.25 mm^3 in the humans based on the resolution of the FA maps) and the smoothing of the warp field and neighborhood correlation radius were the default values (3 voxels and 9 × 9 × 9). This results in a comparable warp field resolution for each set of data acquisition parameters. Obviously relative to the human brain, the macaque monkey brain is roughly 1/12 of the volume (average monkey brain volume 100 cm^3, adult human brain volume 1200 cm^3) and, therefore, our relative voxel resolution is not comparable; however, the monkey data are at the current cutting edge for data acquisition in vivo. Importantly, our measures of variability are within-species numerically, with only the patterns of variability being compared between species, and thus this limitation is only minor in our hands.

Optimal Number of Participants to Build a Template and Reproducibility

The optimal number of participants was calculated producing T1 and FA templates from separate paired populations of equal gender distribution. This approach was repeated for groups consisting of 4, 6, 8, 10, 12, 14, and 16 subjects. Squared spatial Pearson's correlations between each pair (i.e., square of fslcc from FSL) was employed to calculate the percentage of shared variance (i.e., the similarity). Supplementary Figure 1 indicates a steep increase of shared variance between templates produced from T1 and FA maps from 4 to 10 participants followed by a plateau from 10 to 16 participants. This result indicates that, using iterative diffeomorphic deformations, 10 subjects

are sufficient to produce a good enough brain template to match the overall population.

Quantification of the Variability

T1 and FA maps were registered to their corresponding templates and sets of 3 diffeomorphic deformation maps were extracted for each subject corresponding to the orthogonal projection of the deformations for each voxels (i.e., maps *x*, *y*, *z*). Variability was defined as the strength of the deformation (Euclidean distance) required to match each individual map to its corresponding template. The strength of the deformation was calculated for each voxel using the following formula (Gibbs 1881): $| (x, y, z)^T | = \sqrt{(dx^2 + dy^2 + dz^2)}$, where d*x*, d*y*, and d*z* are the difference in each dimension.

Grey Matter Variability

FAST from FSL was employed to extract the grey matter ribbon from the T1 templates and consecutively employed as an inclusion mask to quantify the average grey matter deformation for each subject. Average grey matter deformation was projected on a 3D surface reconstruction using Anatomist (http://brainvisa.info). Surfaces are available on request from the authors.

White Matter Variability

We quantified for every subject the average white matter deformation in each voxel with an FA value > 0.2. Results were projected on the average tractography reconstruction of the human and the monkey dataset (Jones et al. 2002). Average tractography datasets are available on request from the authors.

Brain Size Effect

In order to control for the effect of brain size, we carried out the same estimation using the Jacobian determinant instead of Euclidean distance in order to report the proportional rather than the absolute value of the total deformation required to match the template (Ashburner 2007).

Cortical Folding Effect

The association between surface curvature and morphological variability was estimated using Spearman rank-order correlation (Spearman 1904), and the stability of the results checked using robust regression.

Reproducibility

Reproducibility was assessed in humans using squared spatial Pearson's correlations to estimate the percentage of shared variance between the variability maps derived from the 2 sets of 10 adult healthy controls.

Comparison Between Variability in Humans and Areas of Recent Cortical Expansion

To assess the phylogenetic signature of the morphological variability, we tested the association between the latter and an estimate of cortical expansion in humans compared with monkeys. We employed the macaque-to-human transformation map provided in Caret (http://brainvis.wustl.edu/) (Van Essen and Dierker 2007). This map (Fig. 5 top-right) was calculated by performing a surface-based registration between a macaque monkey and a human brain template. Crucially, the deformation was constrained to align 23 landmarks whose location can be accurately defined across species (e.g., the central sulcus or
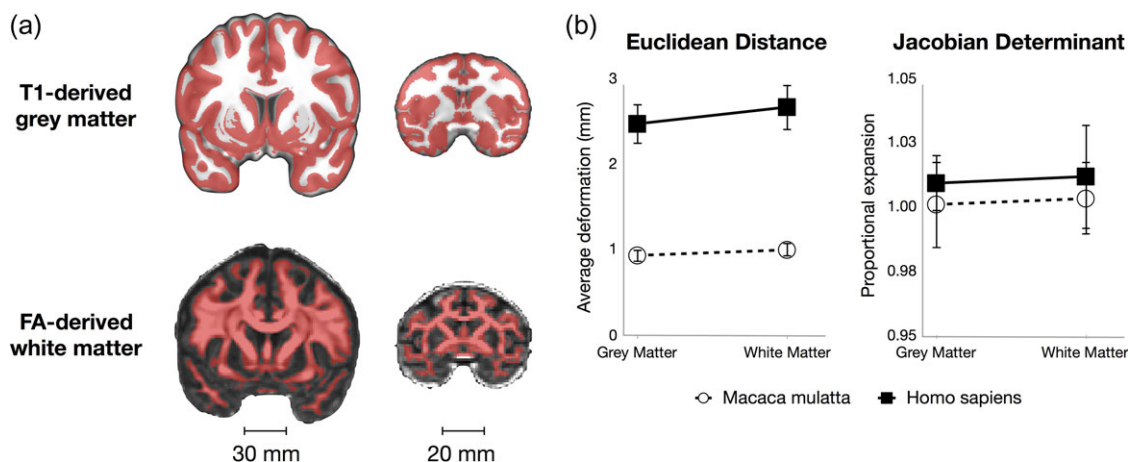
Figure 1. Quantification of the variability. (*a*) T1 and FA maps templates computed for each species. Red indicated the mask used to calculate average deformation. (*b*) Average deformation measured for grey and white matter with standard deviations. The left panel indicates absolute values quantified using Euclidean distance. The right panel indicates relative values estimated by the Jacobian determinant.

the location of the FEF). The geodesic distance between homologous regions within each species would differ not only according to the absolute size of the brain but also according to the different cortical areas separating the regions in either species. For instance, the distance between area MT and A1 is much higher in humans than in monkeys, while the reverse is true for the distance between FEF and the central sulcus (Van Essen 2004a, 2004b). These differences represent an estimate of the differential cortical expansion in humans and monkeys with respect to a common ancestor. For instance, the increased distance between MT and A1 reflects all relative expansion of high-order association cortex in the posterior temporal lobe and STS in humans. For simplicity, we refer here to this deformation map as an "areal expansion map". To assess the relationship between the areal expansion map and our map of anatomical variability in humans, we projected the former onto each cortical voxel in the MNI152 template. We then correlated the values of either maps at each voxel on the cortex. This analysis was performed for each of the five lobes of the brain separately. The association between areal expansion and morphological variability was estimated using Spearman rank-order correlation (Spearman 1904), and the stability of the results was checked using robust regression.

Asymmetries

Asymmetries in humans were quantified using regions of interest defined from the Harvard–Oxford cortical atlas (Zalla et al. 2004; Frazier et al. 2005; Makris et al. 2006; Goldstein et al. 2007). Asymmetries in monkeys were estimated employing regions of interest defined from the INIA19 Primate Brain Atlas (Rohlfing et al. 2012). Human and monkey T1 templates were registered to Harvard and INIA19 Brain atlases respectively and applied to each subject's variability map (i.e., Euclidian distance). An index of asymmetry was consecutively calculated for both species using the following formula:

(Region in the right hemisphere–region in the left hemisphere)/ (region in the right hemisphere + region in the left hemisphere).

Statistics

SPSS 22 software (SPSS, Inc.) was employed to carry out a repeated measure ANOVA with tissue studied (i.e., grey matter and white matter variability) as within-subjects and species (i.e., *Homo sapiens* or *Macaca mulatta*) as between-subjects factors. A one-sample *t*-test approach was applied to quantify the significance of the index of asymmetries for each region investigated. All statistics were Bonferroni corrected for multiple comparisons.

Results

In both species, we analyzed measures of grey (T1-weighted images) and white matter (fractional anisotropy; FA, as measured by diffusion-weighted imaging). By using non-linear deformation-based morphometric analysis, we established the amount of inter-subject variability for both measures, and then compared them between species.

Reproducibility of the Findings

The amount of inter-subject variability for both measures was reproduced in two matched groups of 10 human participants and squared spatial Pearson's correlations indicated a strong shared variance between the variability maps. T1-weighted variability maps shared 92.4% of variance and FA variability maps shared 81.2% of variance. This suggests that the variability maps we calculated with this method are highly reproducible across populations.

Monkey to Human Comparative Variability in Anatomy

The study had a 2 (tissue type: T1 vs. FA) × 2 (species: human vs. monkey) mixed factorial design, which was analyzed with a repeated measure ANOVA revealing significant main effects for tissue type and species (Fig. 1): grey matter (T1) and white matter (FA) express different levels of variability with white matter being much more inconstant than grey matter in both species ($F_{1,28} = 22.272$; $P < 0.001$). The human brain was also statistically more variable than the monkey brain ($F_{1,27} = 385.494$; $P < 0.001$) with a significant interaction between tissue type and species ($F_{1,27} = 5.610$; $P < 0.025$).

When comparing the Jacobian determinant of the grey and white matter deformation, which represents proportional expansion and contraction independent of overall brain size, the human brain was not significantly more variable than the
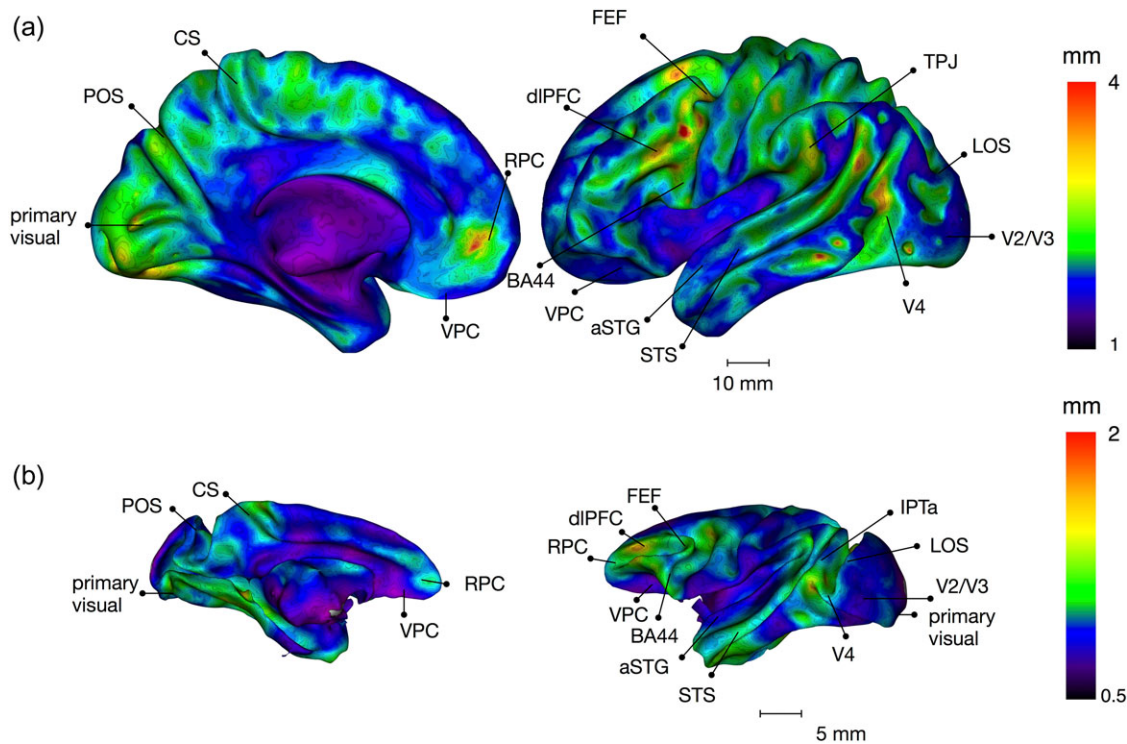
Figure 2. Grey matter variability. Three-dimensional projection of the average deformation measured for grey matter in humans (*a*) and monkeys (*b*). CS, central sulcus; POS, parieto-occipital sulcus; V1, striate cortex; V2, extra striate area 2; V3, extra striate area 3; V4, extra striate area 4; Cereb, cerebellum; VPC, ventral prefrontal cortex; RPC, rostral prefrontal cortex; LOS, lateral occipital sulcus; IPTa, inferior parietal tertiary association cortex; BA44, pars opercularis; FEF, frontal eye field; TPJ, temporo-parietal junction; aSTG, anterior superior temporal gyrus; STS, superior temporal sulcus. Note that since neither a functional nor microscopic delineation of the microscopically or functionally defined cortical areas has been performed in this research, the localization of the functional areas reported in this illustration is an estimate.

monkey brain ($F_{1,27}$ = 2.932; P = 0.098) with no interaction between tissue and species ($F_{1,20}$ = 0.001; P = 0.971) (Fig. 1).

Grey Matter Variability

Both species showed distinct increased variability located in the upper visual field of primary visual area (V1), V4, lateral occipital sulcus (LOS), dorsal parieto-occipital sulcus (POS), middle and posterior parts of the superior temporal sulcus (STS), posterior cingulate sulcus (CS), pars opercularis, frontal-eye-field (FEF), and the rostral prefrontal cortex (RPC) (Fig. 2).

Both species showed lower variability in extra striate visual areas (V2/V3) and ventral prefrontal cortex (VPC). However, while the temporo-parietal junction (TPJ) showed high variability in humans, the equivalent region in monkeys, the mid-STS, did not show similarly high variability. As compared with monkeys, humans showed specifically lower variability in the anterior portion of the lateral prefrontal cortex and a "hot spot" of high variability in the dorsal medial frontal cortex (Fig. 2).

White Matter Variability

Both species showed increased variability in the superficial white matter, which was particularly distinct for the white matter connecting the frontal eye field (FEF), primary motor areas (M1), primary sensory areas (S1) as well as extra striate area 4 (V4) and striate area (V1) (Fig. 3 and Supplementary Figure 2).

Both species showed lower variability in deep white matter structures including for instance, in the core of the corticospinal tract (CST), the cingulum (Cing), the fornix (FX) and the most

medial portion of the inferior longitudinal fasciculus (ILF), and the optic radiations (Fig. 3 and Supplementary Figure 2).

Grey Variability in Humans and Cortical Folding

Analysis of the correlation between grey matter variability findings in humans and surface curvature (Van Essen and Dierker 2007) (Fig. 4) indicated a significant relationship with a small effect size between variability and cortical folding in the left (Spearman's rho = −0.135; $P < 10^{-159}$) the right hemispheres (rho = −0.065; $P < 10^{-36}$).

Grey Variability in Humans and Areas of Recent Cortical Expansion

Analysis of the correlation between grey matter variability findings in humans and macaque-to-human areal expansion (Van Essen and Dierker 2007) (Fig. 5) revealed a significant positive correlation between variability and areal expansion in the temporal lobes and limbic system bilaterally (left temporal lobe, Spearman's rho = 0.403; right temporal lobe, rho = 0.413; left limbic system, rho 0.320; right limbic system, rho = 0.517; $P < 10^{-69}$ in all cases). There was a significant negative correlation in the occipital lobes bilaterally (left occipital lobe, rho = −0.208; right occipital lobe, rho = −0.366; both $P < 10^{-55}$). In the frontal lobes, there was a positive correlation between variability and areal expansion in the left hemisphere (rho = 0.137, $P < 10^{-56}$) but not in the right hemisphere (rho = 0.013, P = 1). In the parietal lobes, there was a positive correlation in the right hemisphere (rho = 0.060, $P < 0.00001$) but not in the left hemisphere (rho = 0.002, P = 0.629).
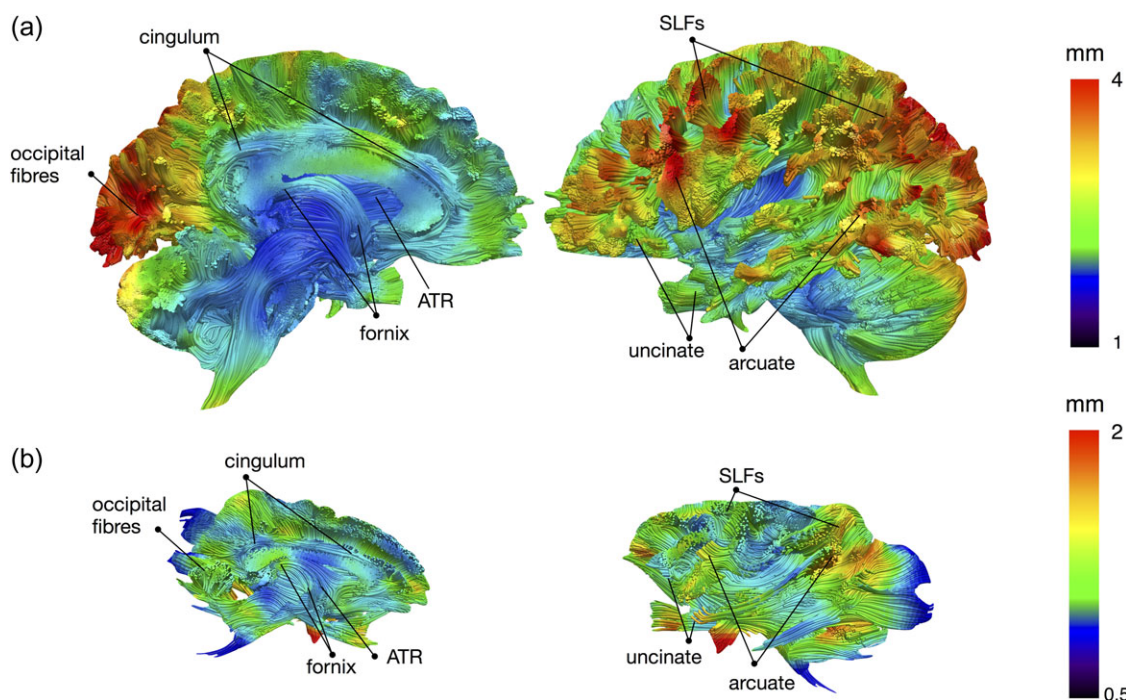
Figure 3. White matter variability. Three-dimensional projection of the average deformation measured for white matter in humans (*a*) and monkeys (*b*). SLFs, branches of the superior longitudinal fasciculus; ATR, anterior thalamic radiation.

Because we found a significant relationship with a small effect size between variability and cortical folding, we repeated the correlation analysis between the grey matter variability findings and areal expansion, this time regressing out the mean cortical curvature measures. Our results remained highly significant with positive partial correlation between variability and areal expansion in the temporal lobes and limbic system bilaterally (left temporal lobe, Spearman's rho = 0.402; right temporal lobe, rho = 0.407; left limbic system, rho 0.311; right limbic system, rho = 0.517; $P < 10^{-65}$ in all cases). There was a significant negative partial correlation in the occipital lobes bilaterally (left occipital lobe, rho = −0.237; right occipital lobe, rho = −0.417; both $P < 10^{-55}$). In the frontal lobes, there was a positive partial correlation between variability and areal expansion in the left hemisphere (rho = 0.130, $P < 10^{-52}$) but not in the right hemisphere (rho = 0.004, $P = 1$). In the parietal lobes, there was a positive partial correlation in the right hemisphere (rho = 0.071, $P < 10^{-7}$) but not in the left hemisphere (rho = 0.025, $P = 0.369$).

Cortical Asymmetries

Results are summarized in Figure 6 and Supplementary Tables 1 and 2. One-sample *t*-tests revealed that, in humans, the Heschl's gyrus ($t_{(19)} = -3.879$; $P = 0.045$) as well as the superior (anterior portion $t_{(19)} = -5.190$; $P = 0.002$; posterior portion $t_{(19)} = -4.798$; $P = 0.006$) and middle (anterior portion $t_{(19)} = -4.978$; $P = 0.004$; middle portion $t_{(19)} = -5.650$; $P = 0.001$) temporal gyri were significantly more variable in the left hemisphere when compared with the right hemisphere. Conversely, the paracingulate ($t_{(19)} = 5.204$; $P = 0.002$) and lingual ($t_{(19)} = 4.861$; $P = 0.005$) gyri were significantly more variable in the right hemisphere.

In monkeys, solely the supramarginal ($t_{(9)} = 6.308$; $P = 0.004$) and angular gyrus ($t_{(9)} = 5.273$; $P = 0.014$) were significantly more variable in the right hemisphere.

Discussion

In this study, we compared the amount of structural variability in the brain across two key species: humans and rhesus macaque monkeys. In addition, we explored the relationship between anatomical variability and areal expansion maps of the primate brain. Four main findings emerge from our work. First, overall, the human brain is not proportionally more variable than that of the monkey, and both species have distinct similarities and differences in grey and white matter variabilities within specific regions. Second, there were some differences between species in specific regions that may underline functional differences between the two species. Third, there was a significant correlation between our anatomical variability maps and the classical maps of evolutionary expansion for most of the lobes of the brain. Finally, the degree of grey matter variability shows significant differences between the left and the right hemispheres in the human brain, and very little difference between the hemispheres in monkeys. Based on these findings, we concluded that variability is a useful measure for comparison between species, and cautiously suggest that this may reveal details about the relative evolutionary hierarchy of specific brain regions across species.

Our first finding revealed that the human brain only showed higher variability than the monkey brain when brain size was not controlled for (Fig. 1). This is perhaps unsurprising given the strong role that brain size plays in primate evolution (Semendeferi et al. 2002; Sherwood et al. 2005) and its proposed relationship with higher-order cognitive functions (Navarrete et al. 2016). In light of the strong relationship between brain structure variability and performance in humans, we may expect brain variability to have a similar relationship with behavior in non-human primates, particularly with regard to complex, recently evolved behavior (Gilissen and Hopkins 2013; Hopkins and Avants 2013; Phillips et al. 2013; Hopkins et al. 2014; Bianchi et al. 2016; Hecht et al. 2016).
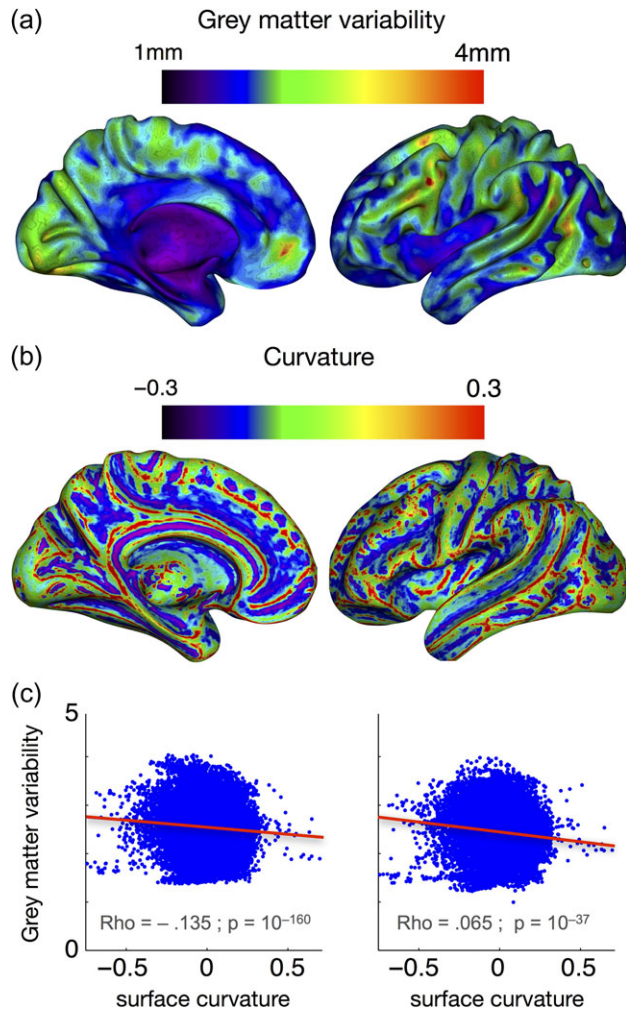
Figure 4. Comparison between grey matter variability (*a*) and cortical folding (*b*) in humans. (*c*) Spearman rho correlations. Results are Bonferroni corrected for multiple comparisons.

Our second finding was that there was regionally specific localization of variability in both species. This was particularly prominent in areas supporting higher-order cognitive function (Fig. 2). For instance, the parieto-occipital sulcus is critically placed to coordinate goal-directed actions in both humans and monkeys, and shows clear homologies between the two species. We also observed high variability in the *pars opercularis* in both species. Cortical stimulation of this area elicits orofacial movements in the primate brain (Huang et al. 1989) and phonemic paraphasia in the human brain (Duffau 2012). The posterior part of the STS in the monkey has been linked to the perception of species-specific vocalizations (Gil-da-Costa et al. 2004) and may be equivalent to Wernicke's area for speech perception and comprehension in humans (Wernicke and Eggert 1874). These areas were highly variable in monkeys and human. The posterior cingulate sulcus, which also was highly variable, is a key hub of the default mode network and is, therefore, implicated in passive or internally oriented tasks in both humans and monkeys (Mantini et al. 2012; Margulies et al. 2016). We also found high variability in the FEFs in both the human and the monkey brain. This complex region is believed to be highly expanded in the primate brain (Elston and Rosa 1998; Hill et al. 2010), notably contributing greatly to the voluntary orienting of

attention, which is a shared function in both humans and monkeys (Buschman and Miller 2007; Mantini et al. 2012). In addition, a number of areas of the rostral prefrontal cortex that are implicated in both positive and negative outcome expectations, as well as outcome monitoring, have shown distinct functional similarities between humans and monkeys (Neubert et al. 2015). Correspondingly, in these areas also, we found high variability in both species.

Areas of low variability within both species were in regions that were less recently evolved and exhibited preserved organization, such as extra striate visual areas (V2/V3), which are largely homologous between humans and monkeys (Van Essen et al. 2001; Orban et al. 2004).

It is important to mention that the pattern of variability follows gross anatomical landmarks to some extent, as demonstrated by the small effect size correlation we found between the grey matter variability and the surface curvature (Fig. 4). This is interesting as a relationship between cortical folding patterns and histologically defined brain areas (Fischl et al. 2008) has been previously reported for some but not all areas in the brain. For instance, primary visual areas are mostly localized in the calcarine sulcus but extend variably to neighboring gyri in humans (Rademacher et al. 1993; Amunts et al. 2000), while there is considerable functional variation between primary visual areas in macaque monkeys (Van Essen et al. 1984). The consistency between cortical folding and cytoarchitectonic fields seems to decrease drastically with the brain hierarchy (Amunts et al. 2007); high-order associative areas being less consistent with sulcal landmarks than primary areas (Fischl et al. 2008). Hence, the variability of this effect across brain areas is consistent with the small effect size of the relationship between variability maps and the cortical folding. This may suggest a complex tripartite relationship between cytoarchitectonic fields, gross anatomical landmarks and inter-individual anatomical variability.

We also identified very specific differences between species in particular grey matter regions (Fig. 2). One difference between the species was a "hot spot" of high variability in dorsal medial frontal cortex, which was not evident in the monkey. Decision-making and abstract reasoning is arguably one of the higher functions of the human brain, allowing humans to imagine an outcome or create a representation of the unchosen option. For example, a region of human dorsal medial frontal cortex associated with the imagining of reward outcomes (Nicolle et al. 2012) did not correspond in a straightforward way to any region of the monkey cortex when comparisons between resting-state functional connectivity patterns were made across species (Neubert et al. 2015). While this region showed high variability in our data for the human brain, there was no clear equivalent in monkey, and is, therefore, consistent with its hypothesized uniqueness in humans. A second difference between the species was in the TPJ, which showed high variability in humans, but the equivalent region in monkeys, the mid-STS (Perrett et al. 1992; Tsao and Livingstone 2008; Pinsk et al. 2009), did not show similarly high variability (Fig. 2). The TPJ has thus shown a great deal of expansion from the monkey to the human brain (Van Essen and Dierker 2007). Despite its putative role in social cognition in monkeys (Sallet et al. 2011; Noonan et al. 2014), the TPJ may process uniquely human attributes of social cognition, such as representing mental states (Saxe 2006; Besharati et al. 2016). The lack of high variability in monkeys may relate to the fact that in our study the monkeys came from a less varied social structure than the humans, but it may also reflect a possible link between the increased role of
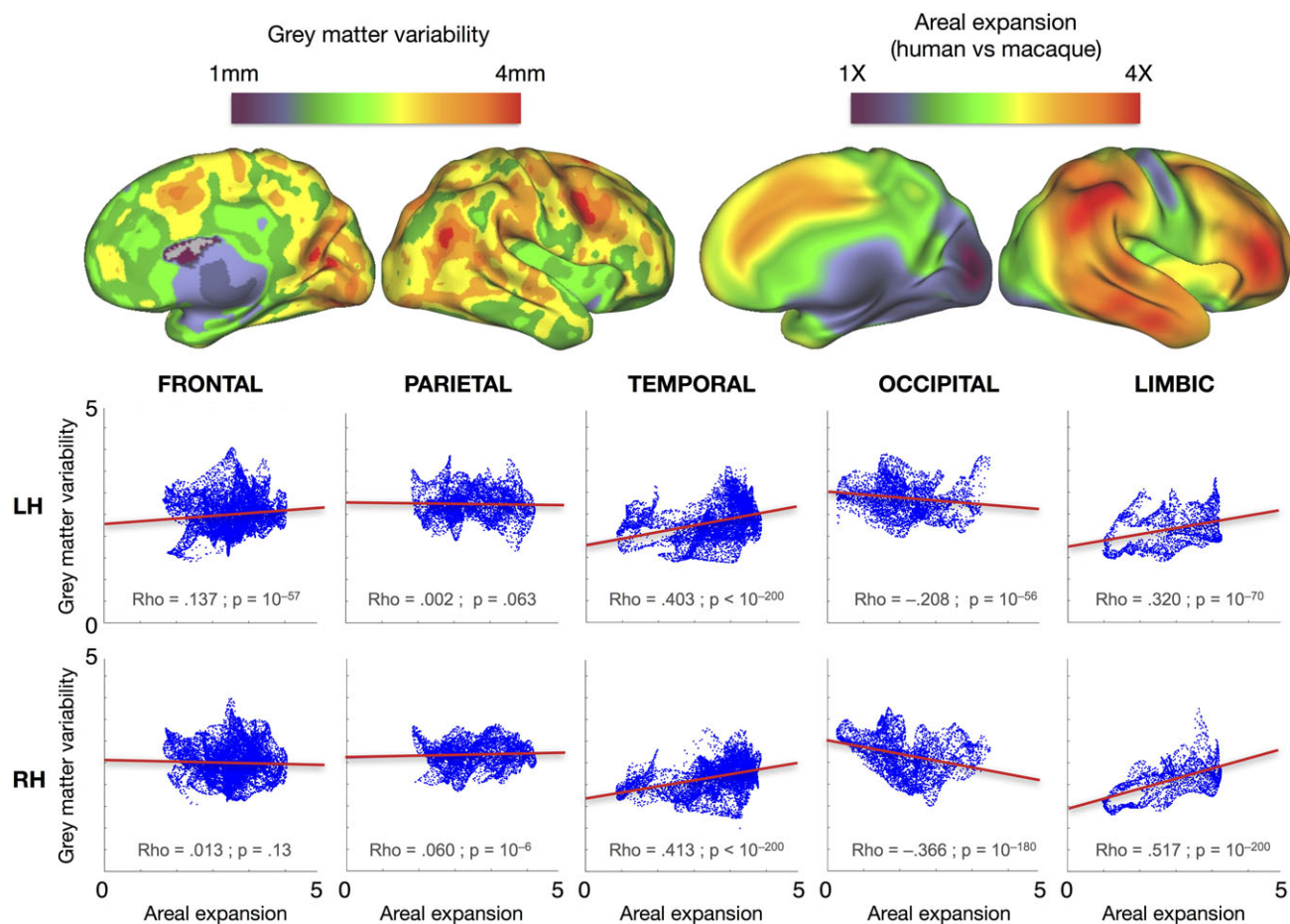
Figure 5. Comparison between grey matter variability in humans and macaque-to-human areal expansion (2). Correlations are shown for each of the major subdivisions of the brain. Spearman rho and P values shown. LH, left hemisphere; RH, right hemisphere. Results are Bonferroni corrected for multiple comparisons.

this region in social cognition and its inter-individual variability in the human brain.

Our third finding was a strong correlation between our grey matter variability maps with previously published evolutionary expansion maps (Van Essen and Dierker 2007) (Fig. 5). This may indicate that the more variable the cortical areas are, the later they may have emerged on the evolutionary tree. Likewise, older, more ancient brain areas tend to be more invariant in their anatomy. The absence of white matter expansion maps in the literature has prevented us from verifying similar principles of white matter variability. Nonetheless, if we assume that there is a strong correlation between the variability and evolutionary expansion maps, our white matter variability maps may constitute an indirect estimate of white matter's phylogenetic dynamic (Fig. 3). These results would suggest that white matter expanded from limbic specific and subcortical areas to later include more associative networks for higher cognitive functions. This interpretation corroborates previous phylogenetic models based on the measure of cortical cytoarchitecture (Yakovlev 1948; Maclean 1949, 1952; Mesulam 2000), neurosurgery (Duffau 2017), and functional connectivity (Margulies et al. 2016), which placed subcortical corticoid and allocortical areas (i.e., limbic zone) at the earliest level of the evolutionary tree followed by the mesocortex (i.e., paralimbic zone) and the isocortex (i.e., idiotopic and homotypical). This phylogenetic gradient is particularly evident on the medial surface of our variability maps (Figs 2 and 3). Similarly, the distribution of

anatomical variability on the lateral surface appears to follow evolutionary trends as depicted by the dual origin hypothesis (Dart 1934; Sanides 1964, 1970; Pandya et al. 2017). According to this hypothesis, brain evolution emerged from two systems, the hippocampocentric and olfactocentric divisions, that meet in the more recently developed regions located in the posterior part of the middle frontal gyrus (supporting, for example, working memory processes, and decision making), posterior temporal lobe (i.e., language comprehension) and inferior parietal lobule (i.e., tool manipulation). We found these areas to be the most variable in terms of their cortical anatomy in the human brain as well as in their subjacent white matter anatomy, recapitulating the gradient suggested by the dual origin hypothesis. However, when interpreting our findings, we consider that we are comparing only two species, each one a product of millions of years of separation and separate evolutionary trajectories. Our findings bear a close resemblance to projected relative evolutionary expansion, and, therefore, may reflect a significant evolutionary finding, but additional species will need to be studied to make a strong conclusion about evolution.

Finally, we investigated the hemispheric differences in variability within the two species (Figure 6). Our findings are broadly consistent with the majority of studies comparing the degree of hemispheric asymmetry between the human and the monkey (Preuss 2011). We noted that the regions of greatest asymmetry were mainly those with the largest degree of hemispheric dominance in humans (Wang et al. 2014). For
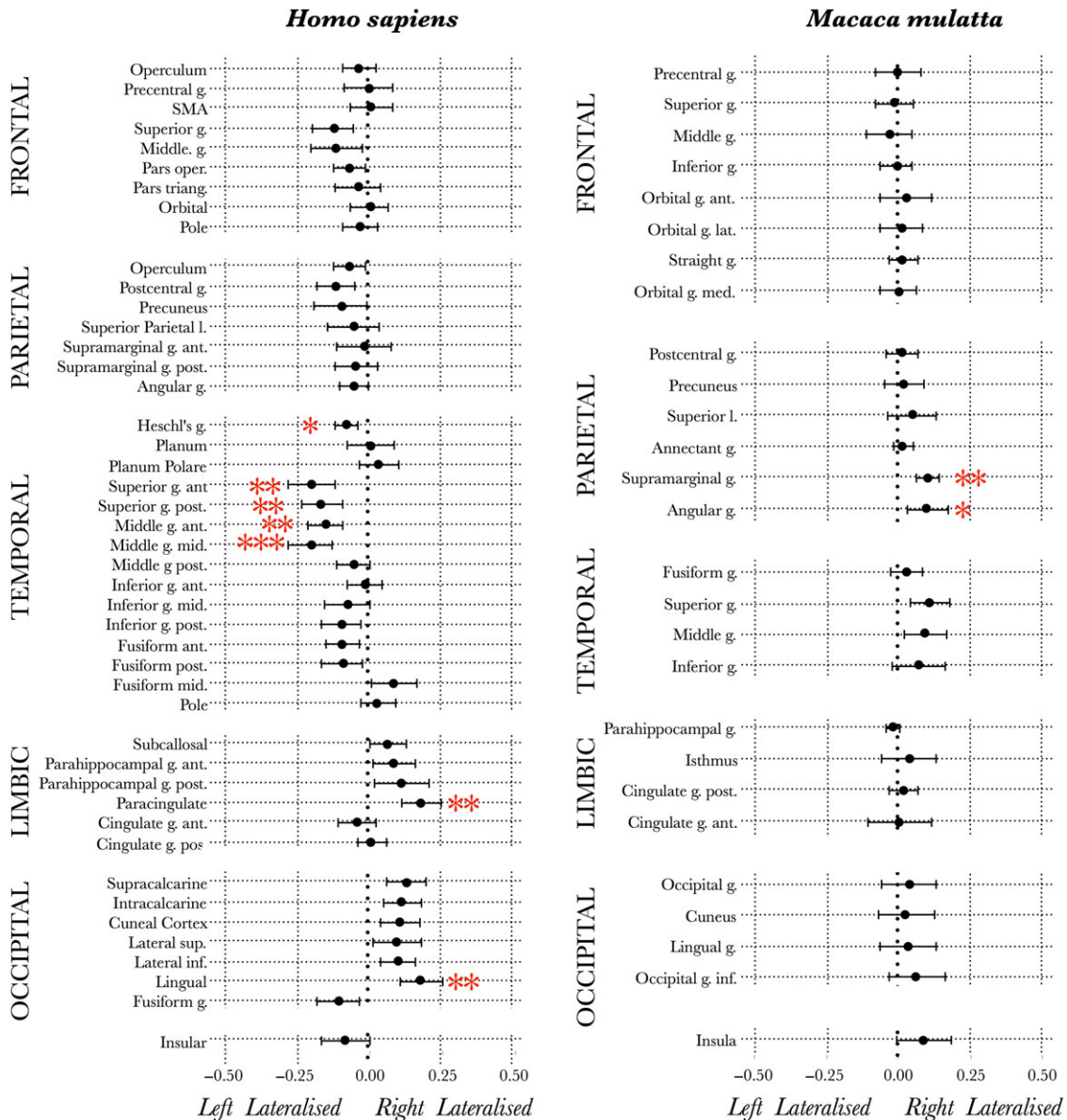
Figure 6. Lateralization indices in grey matter variability in humans (left panel) and monkeys (right panel). Note that the scale for both species is different for visualization purposes. ant., anterior; mid., middle; med., medial; post., posterior; sup., superior; inf., inferior; l., lobule; g., gyrus; SMA, supplementary motor area; oper., opercularis; triang., triangularis. *P < 0.05; **P < 0.01; ***P < 0.001. Results are Bonferroni corrected for multiple comparisons.

instance, language comprehension regions such as Heschl's gyrus and the superior and middle temporal gyri were more variable in the left hemisphere. These results confirm, as previously demonstrated with fMRI (Tzourio-Mazoyer et al. 2015, 2016; Mazoyer et al. 2014), that different brain phenotypes exist to support the phylogenetically recent hemispheric specialization for language in humans. We also noted that the occipital lobe and the paracingulate gyrus were more variable in the right hemisphere than in the left. The paracingulate gyrus is highly variable in humans (Vogt et al. 1995), while the variability in the occipital lobe might be related to interindividual differences in the torque of the occipital lobe (LeMay 1976).

Several factors may have interacted with our findings on variability including genetic diversity, environmental variety, variable personal experiences, and possible evolutionary processes. Differences in image resolution relative to brain size in

humans and monkeys, despite using cutting-edge methodology, may also have contributed to differences and may represent a limitation of our study. However, overwhelmingly, both species showed striking similarities in the pattern of grey and white matter variability, suggesting that the impact of these factors is minimal.

Three key anatomical features may also have confounded our results and represent possible limitations of our study. First, although the size of cytoarchitectonic fields may have remained consistent, an anatomical shift of primary visual areas has caused them to move from the lateral surface to the medial wall along with evolution. This may have differed slightly across subjects and driven the negative correlation between recent macaque-to-human areal expansion and variability we observed in the occipital lobes. Second, an obvious limitation for cortical variability is the degree of inter-subject sulcal variability, for example in the paracingulate, central, or

precentral sulcus (Ono et al. 1990; Vogt et al. 1995; Van Essen 2004a, 2004b). However, we did not generally observe a higher variability in sulci, when compared with gyri or white matter. Third, variation in the macroscopic gyral pattern could also underlie variability (e.g., Retzius 1896; Ono et al. 1990; Thompson et al. 1996; Baare et al. 2001; Yucel et al. 2001). For example, Heschl's gyrus exhibits a highly variable morphology (Brodmann 1909; von Economo and Horn 1930; Celesia 1976; Galaburda and Sanides 1980) that includes 1 to 3 gyri per hemisphere, with the number of gyri varying between hemispheres as well (Pfeifer 1920; von Economo and Horn 1930; Campain and Minckler 1976). Therefore, an alternative explanation for our findings may be that the amount of variation in gyral shape patterns progressively increases across the macaque monkey, chimpanzee, and human brain (Le May and Geschwind 1965; Chen et al. 2013) and may have led to the similarities and differences observed in both human and monkey brain variabilities. Alternatively, variability represents an important additional measure to the anatomical features described above, and may be an important tool for investigating evolutionary differences between species. Future studies will include a wider range of species in order to draw stronger conclusions about the evolutionary significance of structural variability.

Conclusions

Our three most striking findings were the high degree of similarity in variability between humans and monkeys, the strong correlation with macaque-to-human areal expansion maps, and the much greater degree of difference in variability between the hemispheres in humans than in monkeys, in specific functional areas. The latter supports the concept of increased hemispheric specialization in the human brain, potentially one way in which evolution has led to a divergence between the human and monkey. Therefore, it may be that the same variability that makes us individually different from each other is also at the root of our differences from our ancestors and our closest evolutionary relatives. This suggests that cerebral variability may add another dimension to the study of evolutionary mechanisms.

Supplementary Material

Supplementary data are available at *Cerebral Cortex* online.

Funding

Notes

References

Amunts K, Malikovic A, Mohlberg H, Schormann T, Zilles K. 2000. Brodmann's areas 17 and 18 brought into stereotaxic space—where and how variable? NeuroImage. 11:66–84.

Amunts K, Schleicher A, Bürgel U, Mohlberg H, Uylings HB, Zilles K. 1999. Broca's region revisited: cytoarchitecture and intersubject variability. J Comp Neurol. 412:319–341.

Amunts K, Schleicher A, Zilles K. 2007. Cytoarchitecture of the cerebral cortex—more than localization. NeuroImage. 37: 1061–1065. discussion 1066-1068.

Andersson JL, Skare S, Ashburner J. 2003. How to correct susceptibility distortions in spin-echo echo-planar images: application to diffusion tensor imaging. Neuroimage. 20: 870–888.

Andersson JLR, Xu J, Yacoub E, Auerbach E, Moeller S, Ugurbil K. 2012. A Comprehensive Gaussian Process Framework for Correcting Distortions and Movements in Diffusion Images. Melbourne, Australia: ISMRM.

Ashburner J. 2007. A fast diffeomorphic image registration algorithm. NeuroImage. 38:95–113.

Avants B, Gee JC. 2004. Geodesic estimation for large deformation anatomical shape averaging and interpolation. Neuroimage. 23(Suppl 1):S139–S150.

Avants BB, Epstein CL, Grossman M, Gee JC. 2008. Symmetric diffeomorphic image registration with cross-correlation: evaluating automated labeling of elderly and neurodegenerative brain. Med Image Anal. 12:26–41.

Avants BB, Yushkevich P, Pluta J, Minkoff D, Korczykowski M, Detre J, Gee JC. 2010. The optimal template effect in hippocampus studies of diseased populations. Neuroimage. 49: 2457–2466.

Baare WF, Hulshoff Pol HE, Boomsma DI, Posthuma D, de Geus EJ, Schnack HG, van Haren NE, van Oel CJ, Kahn RS. 2001. Quantitative genetic modeling of variation in human brain morphology. Cereb Cortex. 11:816–824.

Barbas H, Pandya DN. 1987. Architecture and frontal cortical connections of the premotor cortex (area 6) in the rhesus monkey. J Comp Neurol. 256:211–228.

Behrens TE, Johansen-Berg H, Woolrich MW, Smith SM, Wheeler-Kingshott CA, Boulby PA, Barker GJ, Sillery EL, Sheehan K, Ciccarelli O, et al. 2003. Non-invasive mapping of connections between human thalamus and cortex using diffusion imaging. Nat Neurosci. 6:750–757.

Besharati S, Forkel SJ, Kopelman M, Solms M, Jenkinson PM, Fotopoulou A. 2016. Mentalizing the body: spatial and social cognition in anosognosia for hemiplegia. Brain. 139:971–985.

Bianchi S, Reyes LD, Hopkins WD, Taglialatela JP, Sherwood CC. 2016. Neocortical grey matter distribution underlying voluntary, flexible vocalizations in chimpanzees. Sci Rep. 6:34733.

Brodmann K. 1909. Vergleichende Lokalisationslehre der Großhirnrinde: in ihren Prinzipien. Leipzig, Germany: Barth.

Budisavljevic S, Dell'Acqua F, Rijsdijk FV, Kane F, Picchioni M, McGuire P, Toulopoulou T, Georgiades A, Kalidindi S, Kravariti E, et al. 2015. Age-related differences and heritability of the Perisylvian language networks. J Neurosci. 35: 12625–12634.

Buschman TJ, Miller EK. 2007. Top-down versus bottom-up control of attention in the prefrontal and posterior parietal cortices. Science. 315:1860–1862.

Campain R, Minckler J. 1976. A note on the gross configurations of the human auditory cortex. Brain Lang. 3:318–323.

Caruyer E, Lenglet C, Sapiro G, Deriche R. 2013. Design of multi-shell sampling schemes with uniform coverage in diffusion MRI. Magn Reson Med. 69:1534–1540.

Catani M, Allin MP, Husain M, Pugliese L, Mesulam MM, Murray RM, Jones DK. 2007. Symmetries in human brain language pathways correlate with verbal recall. Proc Natl Acad Sci USA. 104:17163–17168.

Catani M, Forkel S, Thiebaut de Schotten M. 2010. Asymmetry of the white matter pathways in the brain. In: Hugdahl K, Westerhausen R, editors. The two halves of the brain Cambridge. London: The MIT Press.

Celesia GG. 1976. Organization of auditory cortical areas in man. Brain. 99:403–414.

Chen H, Zhang T, Guo L, Li K, Yu X, Li L, Hu X, Han J, Hu X, Liu T. 2013. Coevolution of gyral folding and structural connection patterns in primate brains. Cereb Cortex. 23:1208–1217.

Croxson PL, Johansen-Berg H, Behrens TE, Robson MD, Pinsk MA, Gross CG, Richter W, Richter MC, Kastner S, Rushworth MF. 2005. Quantitative investigation of connections of the prefrontal cortex in the human and macaque using probabilistic diffusion tractography. J Neurosci. 25:8854–8866.

Dart RA. 1934. The dual structure of the neopallium: its history and significance. J Anat. 69:3–19.

Darwin C 1859. On The Origin Of Species.

Duffau H. 2012. The "frontal syndrome" revisited: lessons from electrostimulation mapping studies. Cortex. 48:120–131.

Duffau H. 2017. A two-level model of interindividual anatomo-functional variability of the brain and its implications for neurosurgery. Cortex. 86:303–313.

Elston GN, Rosa MG. 1998. Complex dendritic fields of pyramidal cells in the frontal eye field of the macaque monkey: comparison with parietal areas 7a and LIP. Neuroreport. 9:127–131.

Fischl B, Rajendran N, Busa E, Augustinack J, Hinds O, Yeo BT, Mohlberg H, Amunts K, Zilles K. 2008. Cortical folding patterns and predicting cytoarchitecture. Cereb Cortex. 18:1973–1980.

Frazier JA, Chiu S, Breeze JL, Makris N, Lange N, Kennedy DN, Herbert MR, Bent EK, Koneru VK, Dieterich ME, et al. 2005. Structural brain magnetic resonance imaging of limbic and thalamic volumes in pediatric bipolar disorder. Am J Psychiatry. 162:1256–1265.

Galaburda A, Sanides F. 1980. Cytoarchitectonic organization of the human auditory cortex. J Comp Neurol. 190:597–610.

Gibbs JW 1881. Elements of vector analysis. New Heaven: Privately Printed.

Gil-da-Costa R, Braun A, Lopes M, Hauser MD, Carson RE, Herscovitch P, Martin A. 2004. Toward an evolutionary perspective on conceptual representation: species-specific calls activate visual and affective processing systems in the macaque. Proc Natl Acad Sci USA. 101:17516–17521.

Gilissen EP, Hopkins WD. 2013. Asymmetries of the parietal operculum in chimpanzees (Pan troglodytes) in relation to handedness for tool use. Cereb Cortex. 23:411–422.

Goldstein JM, Seidman LJ, Makris N, Ahern T, O'Brien LM, Caviness VS Jr., Kennedy DN, Faraone SV, Tsuang MT. 2007. Hypothalamic abnormalities in schizophrenia: sex effects and genetic vulnerability. Biol Psychiatry. 61:935–945.

Hecht EE, Mahovetz LM, Preuss TM, Hopkins WD. 2016. A neuroanatomical predictor of mirror self-recognition in chimpanzees. Soc Cogn Affect Neurosci. 12(1):37–48.

Hill J, Inder T, Neil J, Dierker D, Harwell J, Van Essen D. 2010. Similar patterns of cortical expansion during human development and evolution. Proc Natl Acad Sci USA. 107:13135–13140.

Hopkins WD, Avants BB. 2013. Regional and hemispheric variation in cortical thickness in chimpanzees (Pan troglodytes). J Neurosci. 33:5241–5248.

Hopkins WD, Misiura M, Reamer LA, Schaeffer JA, Mareno MC, Schapiro SJ. 2014. Poor receptive joint attention skills are associated with atypical gray matter asymmetry in the posterior superior temporal gyrus of chimpanzees (Pan troglodytes). Front Psychol. 5:7.

Huang CS, Hiraba H, Murray GM, Sessle BJ. 1989. Topographical distribution and functional properties of cortically induced rhythmical jaw movements in the monkey (Macaca fascicularis). J Neurophysiol. 61:635–650.

Jones DK, Griffin LD, Alexander DC, Catani M, Horsfield MA, Howard RJ, Williams SC. 2002. Spatial normalization and averaging of diffusion tensor MRI data sets. NeuroImage. 17:592–617.

Kaas JH, Stepniewska I. 2015. Evolution of posterior parietal cortex and parietal–frontal networks for specific actions in primates. J Comp Neurol. 524(3):595–608.

Klein A, Andersson J, Ardekani BA, Ashburner J, Avants B, Chiang MC, Christensen GE, Collins DL, Gee J, Hellier P, et al. 2009. Evaluation of 14 nonlinear deformation algorithms applied to human brain MRI registration. NeuroImage. 46:786–802.

Le May M, Geschwind N. 1965. Hemispheric difference in the brains of great apes. Brain Behav Evol. 11:48–52.

LeMay M. 1976. Morphological cerebral asymmetries of modern man, fossil man, and nonhuman primate. Ann N Y Acad Sci. 280:349–366.

Maclean PD. 1949. Psychosomatic disease and the visceral brain; recent developments bearing on the Papez theory of emotion. Psychosom Med. 11:338–353.

Maclean PD. 1952. Some psychiatric implications of physiological studies on frontotemporal portion of limbic system (visceral brain). Electroencephalogr Clin Neurophysiol. 4:407–418.

Makris N, Goldstein JM, Kennedy D, Hodge SM, Caviness VS, Faraone SV, Tsuang MT, Seidman LJ. 2006. Decreased volume of left and total anterior insular lobule in schizophrenia. Schizophr Res. 83:155–171.

Malkova L, Heuer E, Saunders RC. 2006. Longitudinal magnetic resonance imaging study of rhesus monkey brain development. Eur J Neurosci. 24:3204–3212.

Mantini D, Hasson U, Betti V, Perrucci MG, Romani GL, Corbetta M, Orban GA, Vanduffel W. 2012. Interspecies activity correlations reveal functional correspondence between monkey and human brain areas. Nat Methods. 9:277–282.

Margulies DS, Ghosh SS, Goulas A, Falkiewicz M, Huntenburg JM, Langs G, Bezgin G, Eickhoff SB, Castellanos FX, Petrides M, et al. 2016. Situating the default-mode network along a principal gradient of macroscale cortical organization. Proc Natl Acad Sci USA. 113:12574–12579.

Marie D, Jobard G, Crivello F, Perchey G, Petit L, Mellet E, Joliot M, Zago L, Mazoyer B, Tzourio-Mazoyer N. 2015. Descriptive anatomy of Heschl's gyri in 430 healthy volunteers, including 198 left-handers. Brain Struct Funct. 220:729–743.

Mars RB, Jbabdi S, Sallet J, O'Reilly JX, Croxson PL, Olivier E, Noonan MP, Bergmann C, Mitchell AS, Baxter MG, et al. 2011. Diffusion-weighted imaging tractography-based parcellation of the human parietal cortex and comparison with human and macaque resting-state functional connectivity. J Neurosci. 31:4087–4100.

Mars RB, Sallet J, Neubert FX, Rushworth MF. 2013. Connectivity profiles reveal the relationship between brain areas for social cognition in human and monkey temporoparietal cortex. Proc Natl Acad Sci USA. 110:10806–10811.

Mazoyer B, Zago L, Jobard G, Crivello F, Joliot M, Perchey G, Mellet E, Petit L, Tzourio-Mazoyer N. 2014. Gaussian Mixture Modeling of Hemispheric Lateralization for Language in a Large Sample of Healthy Individuals Balanced for Handedness. PLOS ONE. 9(6):e101165. https://doi.org/10.1371/journal.pone.0101165.

Mesulam M. 2000. Behavioral neuroanatomy: large-scale networks, association cortex, frontal syndromes, the limbic system, and hemispheric specializations. In: Mesulam M, editor. Principles of behavioral and cognitive neurology. 2nd ed. New York: Oxford University Press. p. 1–91.

Moeller S, Yacoub E, Olman CA, Auerbach E, Strupp J, Harel N, Ugurbil K. 2010. Multiband multislice GE-EPI at 7 tesla, with 16-fold acceleration using partial parallel imaging with application to high spatial and temporal whole-brain fMRI. Magn Reson Med. 63:1144–1153.

Nathan PW, Smith MC, Deacon P. 1990. The corticospinal tracts in man. Course and location of fibres at different segmental levels. Brain. 113(Pt 2):303–324.

Navarrete AF, Reader SM, Street SE, Whalen A, Laland KN. 2016. The coevolution of innovation and technical intelligence in primates. Philos Trans R Soc Lond B Biol Sci. 371(1690):20150186.

Neubert FX, Mars RB, Sallet J, Rushworth MF. 2015. Connectivity reveals relationship of brain areas for reward-guided learning and decision making in human and monkey frontal cortex. Proc Natl Acad Sci USA. 112:E2695–E2704.

Neubert FX, Mars RB, Thomas AG, Sallet J, Rushworth MF. 2014. Comparison of human ventral frontal cortex areas for cognitive control and language with areas in monkey frontal cortex. Neuron. 81:700–713.

Nicolle A, Klein-Flugge MC, Hunt LT, Vlaev I, Dolan RJ, Behrens TE. 2012. An agent independent axis for executed and modeled choice in medial prefrontal cortex. Neuron. 75:1114–1121.

Noonan MP, Sallet J, Mars RB, Neubert FX, O'Reilly JX, Andersson JL, Mitchell AS, Bell AH, Miller KL, Rushworth MF. 2014. A neural circuit covarying with social hierarchy in macaques. PLoS Biol. 12:e1001940.

O'Reilly JX, Croxson PL, Jbabdi S, Sallet J, Noonan MP, Mars RB, Browning PG, Wilson CR, Mitchell AS, Miller KL, et al. 2013. Causal effect of disconnection lesions on interhemispheric functional connectivity in rhesus monkeys. Proc Natl Acad Sci USA. 110:13982–13987.

Ocklenburg S, Gunturkun O. 2012. Hemispheric asymmetries: the comparative view. Front Psychol. 3:5.

Ono M, Kubik S, Abernathey CD. 1990. Atlas of the cerebral sulci. New York: Thieme.

Orban GA, Van Essen D, Vanduffel W. 2004. Comparative mapping of higher visual areas in monkeys and humans. Trends Cogn Sci. 8:315–324.

Pandya DN, Petrides M, Cipolloni P. 2017. Cerebral cortex: architecture, connections, and the dual origin concept. New York: Oxford University Press.

Passingham RE, Wise R. 2012. The neurobiology of the prefrontal cortex. Oxford: Oxford University Press.

Perrett DI, Hietanen JK, Oram MW, Benson PJ. 1992. Organization and functions of cells responsive to faces in the temporal cortex. Philos Trans R Soc Lond B Biol Sci. 335:23–30.

Pfeifer RA 1920. Myelogenetisch-anatomische untersuchungen ü̈ber das kortikale ende der horleitung. Leipzig.

Phillips KA, Schaeffer JA, Hopkins WD. 2013. Corpus callosal microstructure influences intermanual transfer in chimpanzees. Front Syst Neurosci. 7:125.

Pinsk MA, Arcaro M, Weiner KS, Kalkus JF, Inati SJ, Gross CG, Kastner S. 2009. Neural representations of faces and body parts in macaque and human cortex: a comparative FMRI study. J Neurophysiol. 101:2581–2600.

Preuss TM. 2011. The human brain: rewired and running hot. Ann N Y Acad Sci. 1225(Suppl 1):E182–E191.

Rademacher J, Caviness VS, Steinmetz H, Galaburda AM. 1993. Topographical variation of the human primary cortices: implications for neuroimaging, brain mapping, and neurobiology. Cereb Cortex. 3:313–329.

Retzius G. 1896. Das Menschenhirn. Studien in der makroskopischen Morphologie. Stockholm: Kgl. Buchdr. P. A. Norstedt and Söner.

Rohlfing T, Kroenke CD, Sullivan EV, Dubach MF, Bowden DM, Grant KA, Pfefferbaum A. 2012. The INIA19 template and NeuroMaps Atlas for primate brain image parcellation and spatial normalization. Front Neuroinform. 6:27.

Sallet J, Mars RB, Noonan MP, Andersson JL, O'Reilly JX, Jbabdi S, Croxson PL, Jenkinson M, Miller KL, Rushworth MF. 2011. Social network size affects neural circuits in macaques. Science. 334:697–700.

Sallet J, Mars RB, Noonan MP, Neubert FX, Jbabdi S, O'Reilly JX, Filippini N, Thomas AG, Rushworth MF. 2013. The organization of dorsal frontal cortex in humans and macaques. J Neurosci. 33:12255–12274.

Sanides F. 1964. The cyto-myeloarchitecture of the human frontal lobe and its relation to phylogenetic differentiation of the cerebral cortex. J Hirnforsch. 6:269–282.

Sanides F 1970. Functional architecture of motor and sensory cortices in primates in the light of a new concept of neocortex evolution. In: Noback C, Montagna W, eds. The Primate Brain New York: Appleton-Century-Crofts p 137-208.

Saxe R. 2006. Uniquely human social cognition. Curr Opin Neurobiol. 16:235–239.

Schoenemann PT, Sheehan MJ, Glotzer LD. 2005. Prefrontal white matter volume is disproportionately larger in humans than in other primates. Nat Neurosci. 8:242–252.

Semendeferi K, Lu A, Schenker N, Damasio H. 2002. Humans and great apes share a large frontal cortex. Nat Neurosci. 5:272–276.

Sherwood CC, Bauernfeind AL, Bianchi S, Raghanti MA, Hof PR. 2012. Human brain evolution writ large and small. Prog Brain Res. 195:237–254.

Sherwood CC, Holloway RL, Semendeferi K, Hof PR. 2005. Is prefrontal white matter enlargement a human evolutionary specialization? Nat Neurosci. 8:537–538. ; author reply 538.

Smith SM, Jenkinson M, Woolrich MW, Beckmann CF, Behrens TEJ, Johansen-Berg H, Bannister PR, De Luca M, Drobnjak I, Flitney DE, et al. 2004. Advances in functional and structural MR image analysis and implementation as FSL. NeuroImage. 23:208–219.

Sotiropoulos SN, Jbabdi S, Xu J, Andersson JL, Moeller S, Auerbach EJ, Glasser MF, Hernandez M, Sapiro G, Jenkinson M, et al. 2013. Advances in diffusion MRI acquisition and processing in the Human Connectome Project. Neuroimage. 80:125–143.

Spearman C. 1904. The proof and measurement of association between two things. Am J Psychol. 15:441–471.

Thiebaut de Schotten M, Dell'acqua F, Valabregue R, Catani M. 2012. Monkey to human comparative anatomy of the frontal lobe association tracts. Cortex. 48:82–96.

Thiebaut de Schotten M, ffytche DH, Bizzi A, Dell'Acqua F, Allin M, Walshe M, Murray R, Williams SC, Murphy DG, Catani M. 2011. Atlasing location, asymmetry and inter-subject variability of white matter tracts in the human brain with MR diffusion tractography. Neuroimage. 54:49–59.

Thompson PM, Schwartz C, Lin RT, Khan AA, Toga AW. 1996. Three-dimensional statistical analysis of sulcal variability in the human brain. J Neurosci. 16:4261–4274.

Toga AW, Thompson PM. 2003. Mapping brain asymmetry. Nat Rev Neurosci. 4:37–48.

Tsao DY, Livingstone MS. 2008. Mechanisms of face perception. Annu Rev Neurosci. 31:411–437.

Tzourio-Mazoyer N, Joliot M, Marie D, Mazoyer B. 2015. Variation in homotopic areas' activity and inter-hemispheric intrinsic connectivity with type of language lateralization: an FMRI study of covert sentence generation in 297 healthy volunteers. Brain Struct Funct. 221(5):2735–2753.

Tzourio-Mazoyer N, Perrone-Bertolotti M, Jobard G, Mazoyer B, Baciude M. 2016. Multi-factorial modulation of hemispheric specialization and plasticity for language in healthy and pathological conditions: A review. Cortex. 86:314–339. http://dx.doi.org/10.1016/j.cortex.2016.05.013.

Ugurbil K, Xu J, Auerbach EJ, Moeller S, Vu AT, Duarte-Carvajalino JM, Lenglet C, Wu X, Schmitter S, Van de Moortele PF, et al. 2013. Pushing spatial and temporal resolution for functional and diffusion MRI in the Human Connectome Project. Neuroimage. 80:80–104.

Uylings HB, Rajkowska G, Sanz-Arigita E, Amunts K, Zilles K. 2005. Consequences of large interindividual variability for human brain atlases: converging macroscopical imaging and microscopical neuroanatomy. Anat Embryol (Berl). 210:423–431.

van der Zwan A, Hillen B, Tulleken CA, Dujovny M, Dragovic L. 1992. Variability of the territories of the major cerebral arteries. J Neurosurg. 77:927–940.

Van Essen D, Lewis J, Drury H, Hadjikhani N, Tootell R, Bakircioglu M, Miller M. 2001. Mapping visual cortex in monkeys and humans using surface-based atlases. Vision Res. 41:1359–1378.

Van Essen DC. 2004a. Surface-based approaches to spatial localization and registration in primate cerebral cortex. Neuroimage. 23(Suppl 1):S97–S107.

Van Essen DC. 2004b. Towards a quantitative, probabilistic neuroanatomy of cerebral cortex. Cortex. 40:211–212.

Van Essen DC, Dierker DL. 2007. Surface-based and probabilistic atlases of primate cerebral cortex. Neuron. 56:209–225.

Van Essen DC, Newsome WT, Maunsell JH. 1984. The visual field representation in striate cortex of the macaque monkey: asymmetries, anisotropies, and individual variability. Vision Res. 24:429–448.

Van Essen DC, Newsome WT, Maunsell JH, Bixby JL. 1986. The projections from striate cortex (V1) to areas V2 and V3 in the macaque monkey: asymmetries, areal boundaries, and patchy connections. J Comp Neurol. 244:451–480.

Van Essen DC, Smith SM, Barch DM, Behrens TE, Yacoub E, Ugurbil K, Consortium WU-MH. 2013. The WU-Minn Human Connectome Project: an overview. Neuroimage. 80:62–79.

Vincent JL, Patel GH, Fox MD, Snyder AZ, Baker JT, Van Essen DC, Zempel JM, Snyder LH, Corbetta M, Raichle ME. 2007. Intrinsic functional architecture in the anaesthetized monkey brain. Nature. 447:83–86.

Vogt BA, Nimchinsky EA, Vogt LJ, Hof PR. 1995. Human cingulate cortex: surface features, flat maps, and cytoarchitecture. J Comp Neurol. 359:490–506.

Vogt C, Vogt O. 1919. Ergebnisse unserer hirnforschung. J Psychol Neurol. 25:279–461.

von Economo C, Horn L. 1930. Über Windungsrelief, Maße und Rindenarchitektonik der Supratemporalfla̎che, ihre individuellen und ihre Seitenunterschiede. Z Gesamte Neurol Psychiatrie. 130:678–757.

Wang D, Buckner RL, Liu H. 2014. Functional specialization in the human brain estimated by intrinsic hemispheric interaction. J Neurosci. 34:12341–12352.

Wernicke C, Eggert G 1874. Der Aphasische Symptomencomplex. Ein psychologische Studie auf anatomischer Basis.

Whitaker HA, Selnes OA. 1976. Anatomic variations in the cortex: individual differences and the problem of the localization of language functions. Ann N Y Acad Sci. 280:844–854.

Yakovlev PJ. 1948. Motility, behavior and the brain; stereodynamic organization and neural coordinates of behavior. J Nerv Ment Dis. 107:313–335.

Yucel M, Stuart GW, Maruff P, Velakoulis D, Crowe SF, Savage G, Pantelis C. 2001. Hemispheric and gender-related differences in the gross morphology of the anterior cingulate/paracingulate cortex in normal volunteers: an MRI morphometric study. Cereb Cortex. 11:17–25.

Zalla T, Joyce C, Szoke A, Schurhoff F, Pillon B, Komano O, Perez-Diaz F, Bellivier F, Alter C, Dubois B, et al. 2004. Executive dysfunctions as potential markers of familial vulnerability to bipolar disorder and schizophrenia. Psychiatry Res. 121:207–217.

Zhang D, Guo L, Zhu D, Li K, Li L, Chen H, Zhao Q, Hu X, Liu T. 2013. Diffusion tensor imaging reveals evolution of primate brain architectures. Brain Struct Funct. 218:1429–1450.